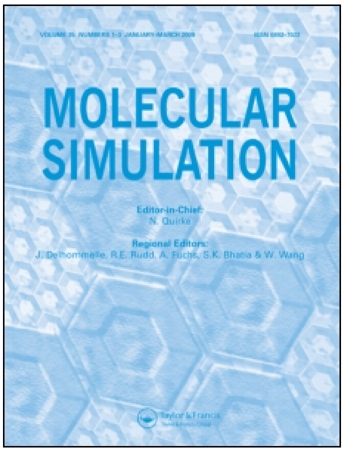

Molecular Simulation
Publication details, including instructions for authors and subscription information:
http://www.informaworld.com/smpp/title~content=t713644482

Interlayer energy-optimum stacking registry for two curved graphene sheets of nanometre dimensions

Yufeng Guo[a]; Wanlin Guo[a]
[a] Institute of Nano Science, Nanjing University of Aeronautics and Astronautics, Nanjing, China

To cite this Article Guo, Yufeng and Guo, Wanlin(2008) 'Interlayer energy-optimum stacking registry for two curved graphene sheets of nanometre dimensions', Molecular Simulation, 34: 8, 813 — 819

To link to this Article: DOI: 10.1080/08927020802294331

URL: http://dx.doi.org/10.1080/08927020802294331

Molecular Simulation
Vol. 34, No. 8, July 2008, 813–819

Taylor & Francis
Taylor & Francis Group

Interlayer energy-optimum stacking registry for two curved graphene sheets of nanometre dimensions

Yufeng Guo* and Wanlin Guo[1]

Institute of Nano Science, Nanjing University of Aeronautics and Astronautics, Nanjing, China

(*Received 18 March 2008; final version received 21 June 2008*)

The interlayer energy between two circular graphene sheets of nanometre scale, which is curved into cylindrical shape with different curvature radius, is investigated by a molecular force field based on a registry-dependent interlayer interaction potential. It is found that there is a special interlayer stacking angle near which the interlayer energy is significantly lower. This interlayer energy-minimum stacking registry angle shifts away from the original Bernal (AB) stacking orientation when the curvature radius of curved graphene sheets is less than 20 nm, and increases with decreasing curvature radius beyond this point. The stability of interlayer energy-minimum stacking of the curved graphene sheets decreases with decreasing curvature radius.

Keywords: curved graphene; interlayer stacking registry; energy-optimum; molecular force field; static calculation

1. Introduction

Graphene sheets of few atomic layers have been discovered recently and exhibit exceptional electronic and transport properties, which may lead to significant advances in semiconductor devices and systems [1–5]. Moreover, synthesised nanoscale graphene-based composite materials have the potential to be excellent electronic materials [6], and the flexible electrical and structural properties of graphene sheets may find relevant applications in nanoelectronics [7].

In particular, the transport and mechanical properties of few-layer graphene sheets strongly depend upon structural stability and interlayer geometry of the stacking of the layers [8,9]. Planar few-layer graphene sheets are usually unstable and could be easily distorted [1,6,10–12]. Previous studies have reported that few-layer graphene sheets were folded by scanning tunnelling microscope, and different folding directions resulted in Bernal (or AB) or hexagonal (or AA) stacking of folded sheets on the graphitic surface [13–15]. In natural graphite, graphene layers are observed to be about 85% in AB stacking and 15% in rhombohedral (or ABC) stacking. Structural deformation in the graphene sheet can significantly influence the interlayer interaction [16–18], so that the corresponding interlayer stacking registry may be different from the planar graphene sheets. Furthermore, with the change of the stacking registry in neighbouring layers, the electronic properties of the curved graphene sheets will be altered as well [19]. The possibility of designing the electronic transport properties of graphene sheets by modifying the stacking configurations of neighbouring layers offers a promising method to create flexible electronic nanoscale systems. Another form of graphene sheets, multi-walled carbon nanotubes, have recently been found to exist, the interlayer energetically optimum chiral configurations between neighbouring layers [20]. However, the effects of curvature deformation on the interlayer stacking registry of the few-layer graphene sheets remain to be explored.

In this study, the interlayer interaction and stacking registry between two curved nanoscale graphene sheets have been systematically investigated by molecular statics calculations based on a recently developed registry-dependent potential. The original AB stacking remains the energetically favourable stacking manner between two slightly curved graphene layers. A slight shift in the registry angle from the original AB stacking orientation occurs to achieve the minimum or optimum interlayer energy when the sheets are curved beyond a critical curvature radius about 20 nm. This shift in the energy-optimum registry angle increases with the decreasing curvature radius of the graphene sheets.

2. Method and model

The interlayer interaction in the layered graphitic sheets is dominated by the long-ranged van der Waals (vdW) interaction. Many *ab initio* quantum mechanical methods such as density function theory (DFT) do not explicitly account for the long-ranged vdW interaction, and large-scale simulations of nanoscale systems are still difficult by quantum mechanical calculations. Therefore, empirical

---

*Corresponding author. Email: yfguo@nuaa.edu.cn

ISSN 0892-7022 print/ISSN 1029-0435 online

DOI: 10.1080/08927020802294331
http://www.informaworld.com

methods capable of predicting both the energy level at the vdW distance as well as the equilibrium distance are necessary for studying the interlayer interaction of large graphitic systems. Recently, Kolmogorov and Crespi [16–18] have developed a registry-dependent interlayer interaction potential, which is specifically parameterised according to the results of DFT and experiments for layered carbon structures, or the K–C potential:

$$V(\vec{r}_{ij},\vec{n}_i,\vec{n}_j) = \mathrm{e}^{-\lambda(r_{ij}-z_0)}[C+f(\rho_{ij})+f(\rho_{ji})] - A\left(\frac{r_{ij}}{z_0}\right)^{-6},$$

$$\rho_{ij}^2 = r_{ij}^2 - (\vec{n}_i\vec{r}_{ij})^2,$$

$$\rho_{ji}^2 = r_{ij}^2 - (\vec{n}_j\vec{r}_{ij})^2,$$

$$f(\rho) = \mathrm{e}^{-(\rho/\delta)^2}\sum C_{2n}(\rho/\delta)^{2n}. \qquad (1)$$

where $\vec{r}_{ij}$ and r_{ij} are the distance vector and the nonbonding interatomic distance, $\vec{n}_i, \vec{n}_j$ are the normal vectors. The function f, which reflects the directionality of the overlap, rapidly decays with the transverse distance ρ [18]. The K–C potential contains a vdW attraction and an exponentially decaying repulsion due to the interlayer wave-function overlap. This potential provides a better description than Lennard-Jones potential in the registry dependent interlayer interaction of adjacent flat and curved graphene layers, and can properly predict the interlayer energy and equilibrium interlayer distance of 0.334 nm for graphite [16–18,20–22].

In this study, we chose two circular-shaped graphene sheets of a diameter $D = 16$ nm, which are cut from two big graphene sheets, as shown in Figure 1. The circular graphene sheets include approximately 15,355 carbon atoms with initial AB stacking orientation. The initial length of the carbon bond of the graphene sheets is 0.142 nm. The graphene sheet of circular shape is selected to avoid the change in overlap area, and the larger diameter is selected to mitigate the boundary effects. The bilayer model is appropriate because the interaction energy between two non-adjacent layers is at least 50 times lower than those between two adjacent layers [20]. The intralayer configuration and structure of the graphene sheets are fully relaxed by the total energy minimisation method using Tersoff–Brenner potential [23]. Then, to study the interlayer interaction of different stacking registry, both the inner and outer layers of the graphene sheets are rotated around the sheets centre O_c with two different angles (registry angles) of θ_i and θ_o from the curving axis (dash line), as shown in Figure 1. When θ_i equals θ_o, the graphene sheets remain in the initial AB stacking orientation. In order to study ideal curvature effects on the interlayer interaction, the graphene sheets are artificially curved into a cylindrical shape along the initial axis (dash line in Figure 1) with a curvature radius R of inner layer. The intralayer atomic configuration and bond length are fixed and remain unchanged, and the arc length of the curved sheets remains at the initial length of 16 nm when the graphene sheets are curved into different curvature radius.

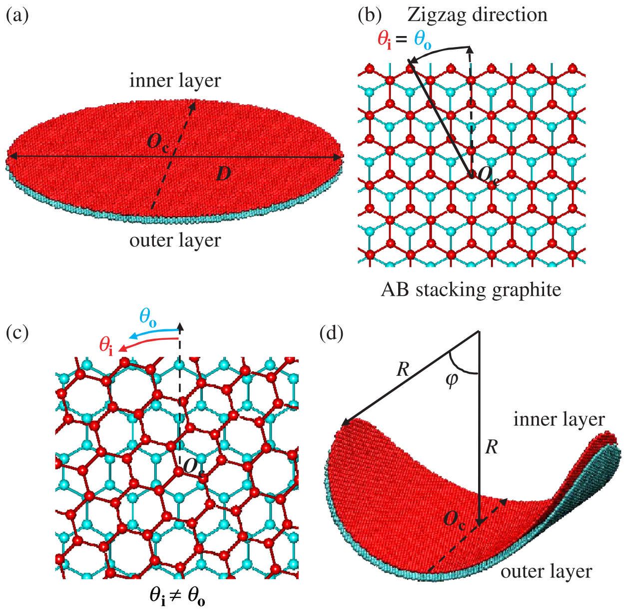

Figure 1. Curving two circular-shaped graphene sheets. (a) Initial AB stacking planar graphene sheets with a diameter $D = 16$ nm. (b) and (c) The adjacent inner and outer graphene layers are rotated around the centre O_c and curving axis (dash line) of the graphene sheets with two different angles θ_i and θ_o. The graphene sheets are curved along the axis (dash line) into (d) state with a relative angle of φ and a curvature radius of R. The curving axis remains unchanged and represents the initial zigzag direction (colour online).

For a given registry angle of the outer layer θ_o, the inner layer is firstly rotated to different θ_i with a very fine step of 0.01°, then the whole sheets are curved to a selected curvature radius R along the curving axis. At each rotation step, the structure of the curved graphene sheets is fixed and the corresponding nonbonding interaction potential energy between the adjacent curved graphene sheets is calculated by using a molecular force field based on the K–C potential.

3. Results and discussion

When the graphene sheets are curved as shown in Figure 1, the original distance and orientation between stacked atoms in the adjacent layers are changed by the curvature deformation. For a given registry angle of the outer layer θ_o, the interlayer interaction energy between the graphene layers mainly depends on the interlayer distance ΔR, curvature radius R and inner layer rotation angle θ_i. Figure 2 gives the variations of the interlayer potential energy with θ_i of $\theta_o = 0°$. For the flat graphene sheets of different

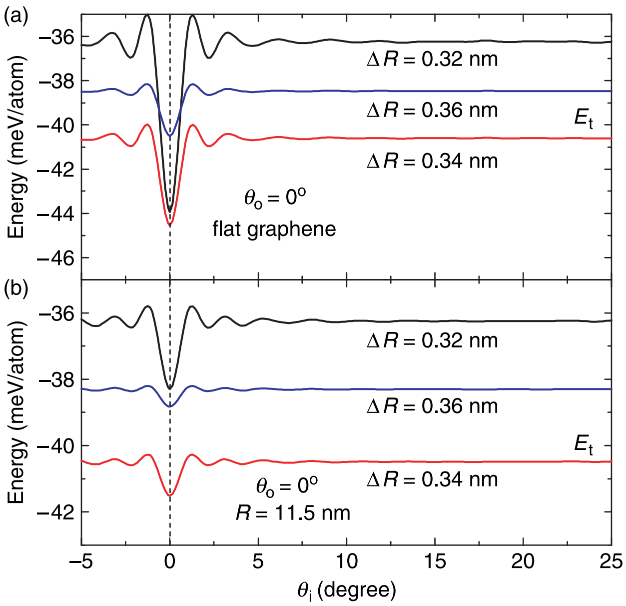

Figure 2. Variations of interlayer energy versus the inner layer registry angle θ_i for the outer layer angle $\theta_o = 0°$ in (a) the flat sheet and (b) a curvature radius $R = 11.5$ nm with different interlayer distance ΔR. Here, E_t denotes the threshold energy, which is described in the text (colour online).

interlayer distance ΔR, the interlayer energy minimum points θ_i^m are all located at 0°, as shown in Figure 2(a). Here the minimum energy indicates a stable interlayer stacking registry in the graphene sheets, but the magnitude of minimum energy varies with the change of interlayer distance. When the graphene sheets are curved to $R = 11.5$ nm, the minimum interlayer energy is still at $\theta_i^m = 0°$, as shown in Figure 2(b). Curving the sheets along the zigzag direction, the AB stacking is always the energy-minimum or energy-optimum interlayer stacking registry. For $\theta_o = 16°$, the AB stacking ($\theta_i^m = \theta_o = 16°$) is still the energetically favourable interlayer registry in the flat sheets, as shown in Figure 3(a). However, the best matching θ_i^m with the minimum energy becomes slightly larger than θ_o when the sheets are curved to a smaller radius of curvature 11.5 nm (Figure 3(b)).

To investigate the influence of curvature deformation on the equilibrium interlayer distance, the variations of minimum interlayer energy with interlayer distance in the curved graphene sheets for $\theta_o = 0$ and 16° are plotted in Figure 4. At different curvature radius R, the interlayer energy with an interlayer distance of 0.334 nm is the lowest, as shown in Figure 4, although the curvature deformation changes the magnitude of the interlayer energy. The distance of 0.334 nm then can be considered as the equilibrated interlayer distance for the curved graphene sheets. We have also studied other interlayer stacking of $\theta_o = 8$ and 24°, and found the distance of 0.334 nm is the equilibrated interlayer distance in those cases.

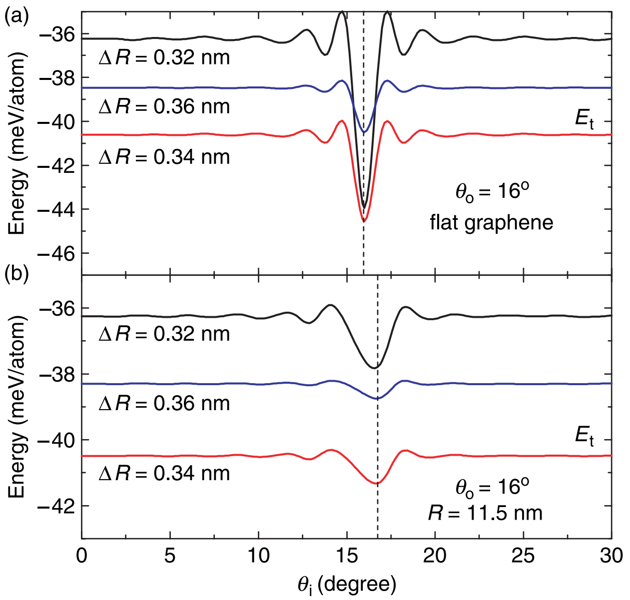

Figure 3. Variations of interlayer energy versus the inner layer registry angle θ_i for the outer layer angle $\theta_o = 16°$ in (a) the flat sheet and (b) a curvature radius $R = 11.5$ nm with different interlayer distance ΔR. Here, E_t denotes the threshold energy (colour online).

According to the minimum interlayer energy of $\theta_o = 0$, 8, 16 and 24°, the relative angle or the difference between the best matching inner-layer registry angle θ_i^m and outer-layer registry angle θ_o, against R for the

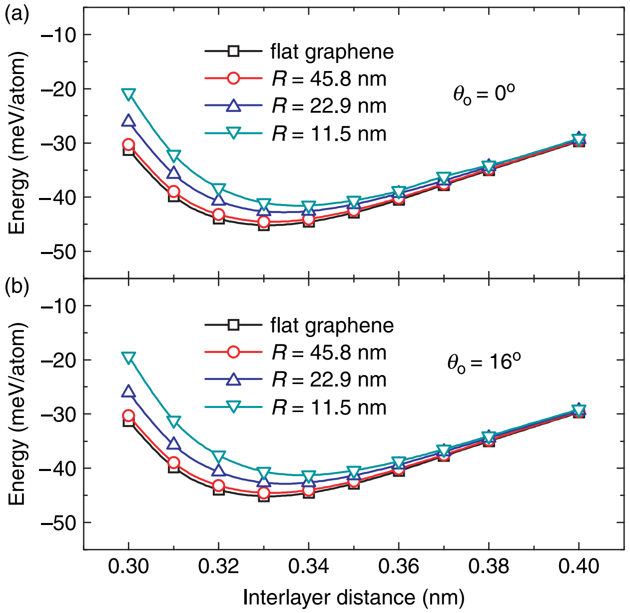

Figure 4. The minimum interlayer energy with interlayer distance of the bilayer graphene sheets at different curvature radius R for (a) $\theta_o = 0°$ and (b) $\theta_o = 16°$ (colour online).

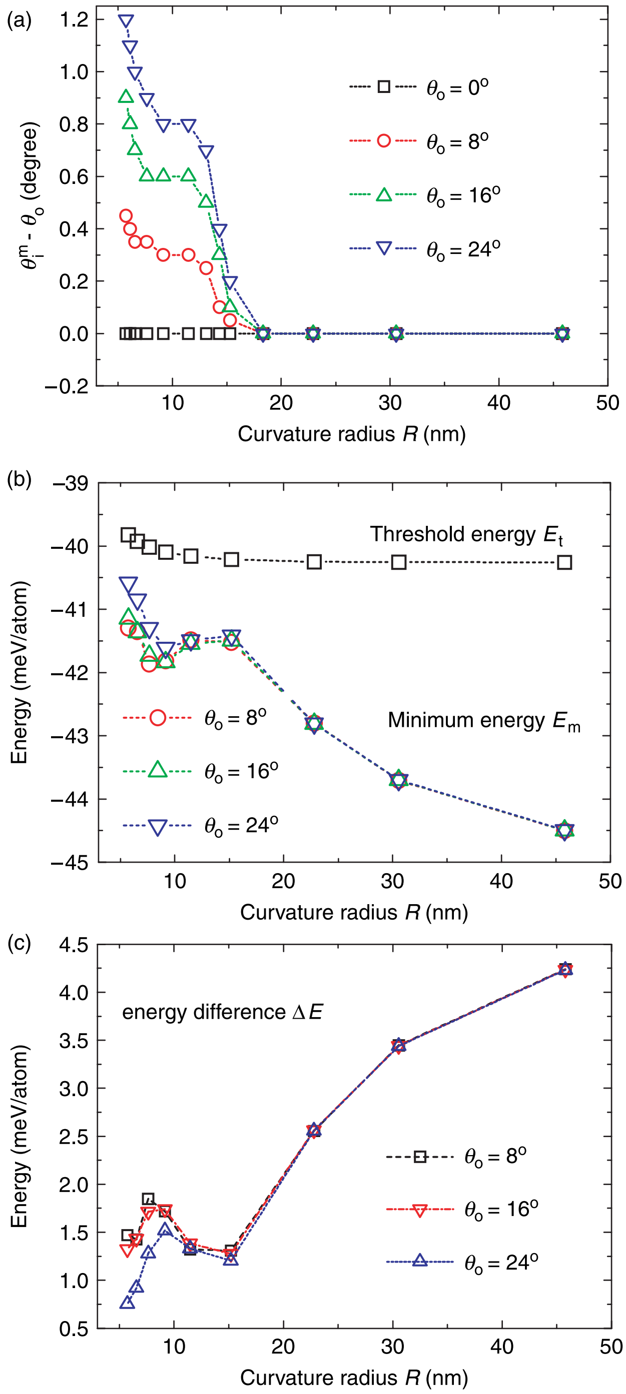

Figure 5. (a) The difference between the energy-minimum inner-layer registry angle θ_i^m and outer-layer registry angle θ_o for the curved $\Delta R = 0.334$ nm graphene sheets, with the curvature radius R for different θ_o. (b) The threshold energy E_t and the minimum interlayer energy E_m with curvature radius of the curved $\Delta R = 0.334$ nm graphene sheets. (c) The corresponding energy difference ΔE between the threshold interlayer energy and the minimum interlayer energy (colour online).

interlayer distance $\Delta R = 0.334$ nm is drawn in Figure 5(a). For $\theta_o = 0°$, the minimum interlayer energy locates at the point of $\theta_i^m = \theta_o = 0°$ when the sheets are curved, so the AB stacking remains the stacking of optimum energy. The cylindrical graphene sheets of $\theta_i^m = \theta_o = 0°$ are similar to a part of a zigzag multi-walled carbon nanotube. This minimum interlayer energy state is consistent with previous study that zigzag multi-walled carbon nanotubes have the minimum interlayer energy [20]. For other cases, the best matching inner-layer registry angle θ_i^m equals to θ_o when the radius of curvature R is larger than about 20 nm. However, when the sheets are further curved to a curvature radius smaller than 20 nm, the best matching θ_i^m becomes larger than θ_o and the difference $\theta_i^m - \theta_o$ increases sharply with decreasing curvature radius. It can be also seen from Figure 5(a) that the difference $\theta_i^m - \theta_o$ increases with increasing θ_o. Larger curvature deformation not only alters the interlayer interaction but also leads to the change of the best matching registry angle for the graphene layers.

As mentioned above when the graphene sheets are curved into cylindrical shape, the curvature deformation changes the original distances between stacked atoms in the adjacent sheets. As a result, the interlayer atomic stacking for $\theta_o = 8$, 16 and 24° cases in the curved graphene sheets is different from that in the flat sheets. A stacking with shifted angles may have the minimum interlayer energy in the curved sheets. This can be seen as the main contribution for the change of best matching registry when the graphene sheets are curved. For $\theta_o = 0°$, the graphene axis is the same as the curving axis, and the interlayer stacking $\theta_i^m = \theta_o = 0°$ remains the minimum interlayer energy.

For the given outer layer angle θ_o, it is found that except a small range of the inner layer registry angle θ_i with lower interlayer potential energy, all other θ_i have a higher and similar interlayer potential energy, as shown in Figures 2 and 3. Here, we define the average value of the interlayer potential energies of which θ_i is 5° away from θ_i^m, as a threshold interlayer energy E_t. The threshold energy reflects the average interlayer interaction between two adjacent graphene layers with arbitrary stacking. While the minimum interlayer energy E_m shown in Figures 2 and 3 can be seen as interlayer cohesive energy of the graphene sheets. Figure 5(b) presents the variations of the threshold energy E_t and the minimum interlayer energy E_m with the radius of curvature R. The threshold energy E_t has the same value for different θ_o, and it decreases with increasing radius R. When the radius R is larger than 20 nm, the threshold energy approaches to a constant value of −40.3 meV/atom. The minimum interlayer energy E_m decreases more sharply with increasing curvature radius. When the radius R is large enough, E_m approaches to the limit value of −45.1 meV/atom in the AB stacking flat graphene sheets. This is in the range of experimental values of natural graphite layers [24–26].

The energy difference ΔE between the threshold energy and the minimum interlayer energy ($\Delta E = E_t - E_m$) is plotted in Figure 5(c). The energy difference ΔE for larger curvature radius is much higher than that for smaller curvature radius. Higher energy difference means that the structure of the best matching outer/inner layers is more stable and energetically favourable. The curvature deformation changes the interlayer interaction, and the energy difference ΔE gradually decreases with decreasing curvature radius of the curved graphene sheets. So the stability of such interlayer energy-minimum sheet decreases with the decreasing curvature radius as well. As a result, the AB or ABC planar stacking graphene sheets are most stable, while the probability of obtaining curved graphene sheets with the interlayer energy-minimum registry becomes lower when it is curved into smaller curvature radius.

In reality, the interlayer spacing of graphene sheets may be varied from the equilibrated distance because of environmental influence and external loading. To understand the effect of interlayer distance change, Figure 6 shows the difference between the best matching registry angle θ_i^m and θ_o for the bilayer graphene sheets with different interlayer distance ΔR. When the curvature radius R is smaller than 18 nm, the best matching outer/inner registry angle difference increases with decreasing curvature radius. Slight differences are found in the variations of $\theta_i^m - \theta_o$ as the interlayer distance ΔR decreases from 0.36 to 0.32 nm. The effects of interlayer distance in the curved graphene sheets slightly change the registry and its curvature-dependence. However, smaller or larger interlayer distance significantly changes the energy value, as shown in Figure 7. Both the threshold energy E_t and the minimum interlayer energy E_m of the distance 0.334 nm are much lower than that of other interlayer distance. Moreover, the energy difference ΔE between E_t and E_m at the same curvature radius increases with the interlayer distance decreasing. The probability of obtaining curved graphene sheets with the optimum registry strongly depends on the energy difference ΔE. Therefore, smaller interlayer distance will lead to a higher probability of realising the best matching registry for the curved graphene sheets.

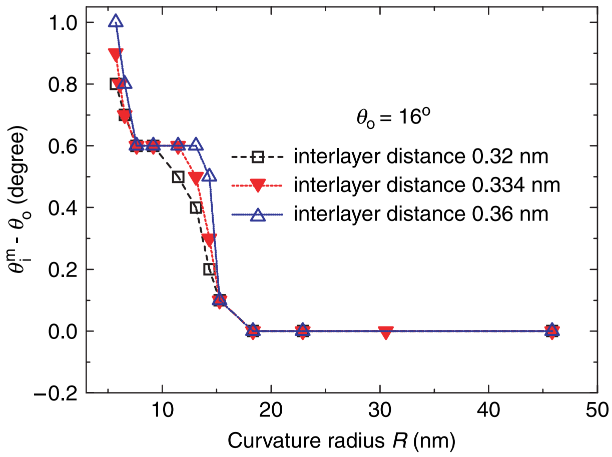

Figure 6. The difference between inner and outer energy-minimum matching registry angles with the curvature radius R of the curved graphene sheets, for different interlayer distance (colour online).

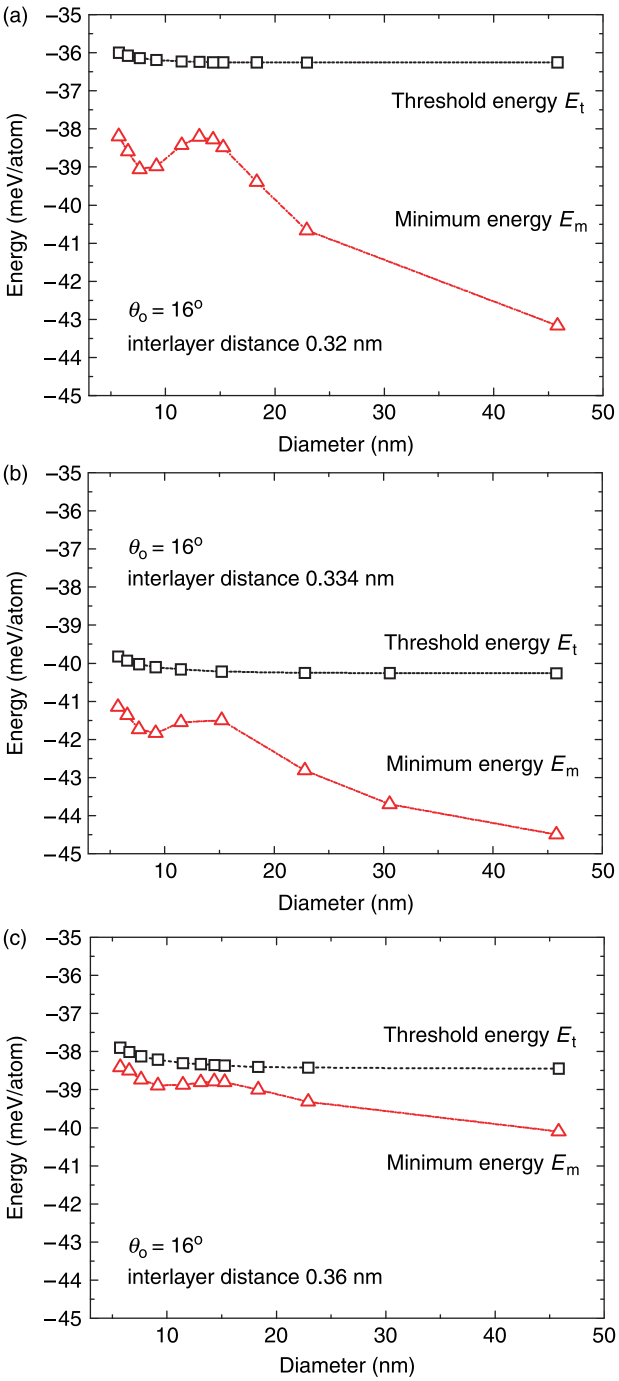

Figure 7. The threshold energy E_t and the minimum interlayer energy E_m of the curved graphene sheets with interlayer distance ΔR of (a) 0.32 nm, (b) 0.334 nm and (c) 0.36 nm (colour online).

In our calculations, the boundaries of the circular graphene sheets are free. Carbon atoms in the boundaries have dangling bonds, which may affect the interlayer energy. The boundary effects are then mainly determined by the dangling bonds. The number of dangling bonds depends on the size of the graphene sheets, and it increases with increasing the diameter D. To study the effects of boundary conditions, we have compared the interlayer interaction of four bilayer graphene sheets with different diameter D. Figure 8 plots the relative angle between the best matching registry angle θ_i^m and θ_o, $\theta_i^m - \theta_o$ for the curved graphene sheets of $D = 17$, 16, 15 and 12 nm. For $D = 12$ nm, the best matching inner-layer registry angle θ_i^m is different from that of larger diameters when the curvature radius is smaller than 18 nm. On the contrary, the curves of $D = 15$, 16 and 17 nm are almost the same. Figure 9 shows the effects of different boundaries on the interlayer energy. There are only slight differences found in the variations of the threshold energy and minimum interlayer energy when the sheet diameter is larger than 15 nm. The contribution of dangling bonds in the boundaries to total interlayer energy gradually decreases with increasing the sheet size. This indicates that the free boundaries in large size graphene sheets will slightly influence the interlayer interaction. According to the results shown in Figures 8 and 9, the graphene sheet diameter of 16 nm chosen in our calculations is large enough to avoid the boundary effects. We have also studied other cases of $\theta_o = 8°$ and 24°, and found that the main results are similar to that of $\theta_o = 16°$.

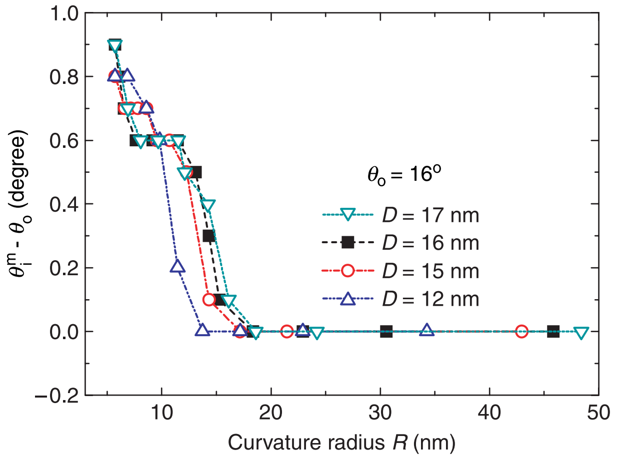

Figure 8. The difference between inner and outer energy-minimum matching registry angles with the curvature radius R of the $\Delta R = 0.334$ nm curved graphene sheets for different diameter D (colour online).

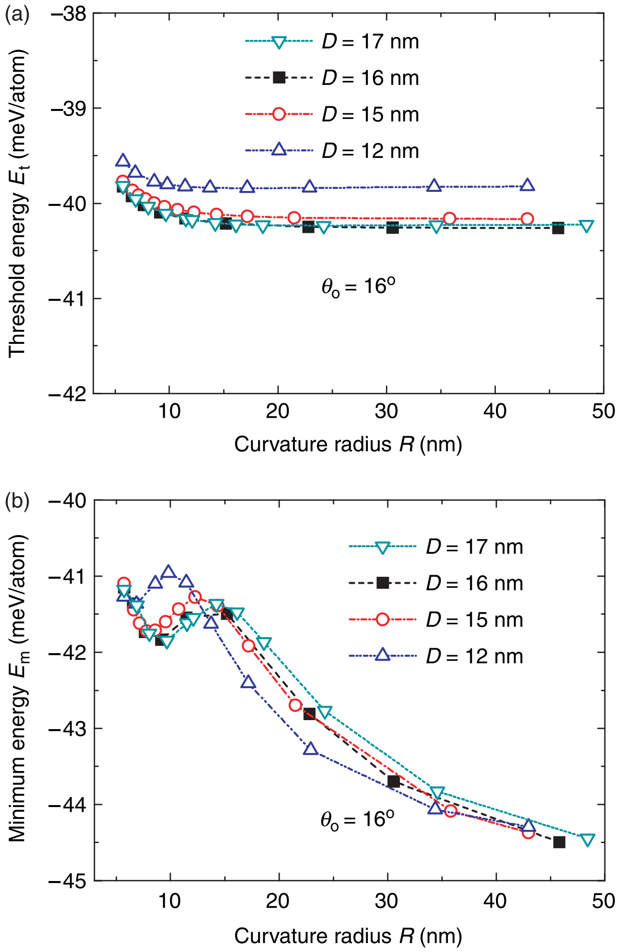

Figure 9. (a) The threshold energy E_t and (b) minimum interlayer energy E_m of the curved $\Delta R = 0.334$ nm graphene sheets with the diameter $D = 12$, 15, 16 and 17 nm (colour online).

4. Conclusion

In summary, the registry structure between two adjacent graphene sheets is immune to slight mechanical distortion according to the present interlayer interaction energy analyses. The AB stacking orientation is always energetically favourable when the sheets are curved along the zigzag direction. However, when the sheets are curved along other direction to a curvature radius smaller than about 20 nm, the initial AB stacking orientation is no longer interlayer energy favourable. The interlayer relative angle between the inner and outer energy-optimum registry angles increases with decreasing curvature radius. Variation in the interlayer distance between two adjacent graphene layers can significantly change the interlayer energy but has very weak influence on the energy-minimum matching registry. The energy difference between the interlayer energy with the optimum registry and the interlayer energies for arbitrary registries decreases with decreasing curvature radius. This means that the registry structural stability becomes weaker for smaller roll of the graphene sheets. These curvature-related registry structures may provide some new insights into fundamental properties of few-layer graphene sheets of nanometre dimensions.

Acknowledgements

The work is supported by the 973 Program (2007CB936204), the Ministry of Education (No. 705021, IRT0534), National NSF, Jiangsu Province NSF (No. BK2006185, BK2005217), Post-doctoral Fund (No. 20060390934) of China and NUAA Innovation Fund. We thank Prof. C.Q. Ru in University of Alberta and Changfeng Chen in Nevada University at Las Vegas for their help.

Note

1. Email: wlguo@nuaa.edu.cn

References

[1] K.S. Novoselov, A.K. Geim, S.V. Morozov, D. Jiang, Y. Zhang, S.V. Dubonos, I.V. Grigorieva, and A.A. Firsov, *Electric field effect in atomically thin carbon films*, Science 306 (2004), p. 666.

[2] K.S. Novoselov, A.K. Geim, S.V. Morozov, D. Jiang, M.I. Katsnelson, I.V. Grigorieva, S.V. Dubonos, and A.A. Firsov, *Two-dimensional gas of massless dirac fermions in graphene*, Nature 438 (2005), p. 197.

[3] Y. Zhang, Y.W. Tan, H.L. Stormer, and P. Kim, *Experimental observation of the quantum Hall effect and Berry's phase in graphene*, Nature 438 (2005), p. 201.

[4] V.M. Pereira, F. Guinea, J.M.B. Lopes dos Santos, N.M.R. Peres, and A.H. Castro Neto, *Disorder induced localized states in graphene*, Phys. Rev. Lett. 96 (2006), p. 036801.

[5] C.L. Kane and E.J. Mele, *Quantum spin Hall effect in graphene*, Phys. Rev. Lett. 95 (2005), p. 226801.

[6] S. Stankovich, D.A. Dikin, G.H.B. Dommett, K.M. Kohlhaas, E.J. Zimney, E.A. Stach, R.D. Piner, S.T. Nguyen, and R.S. Ruoff, *Graphene-based composite materials*, Nature 442 (2006), p. 282.

[7] R.V. Noorden, *Moving towards a graphene world*, Nature 442 (2006), p. 228.

[8] S. Latil and L. Henrard, *Charge carriers in few-Layer graphene films*, Phys. Rev. Lett. 97 (2006), p. 036803.

[9] F. Guinea, A.H.C. Neto, and N.M.R. Peres, *Electronic states and Landau levels in graphene stacks*, Phys. Rev. B 73 (2006), p. 245426.

[10] E. Dujardin, T. Thio, H. Lezec, and T.W. Ebbesen, *Fabrication of mesoscopic devices from graphite microdisks*, Appl. Phys. Lett. 79 (2001), p. 2474.

[11] A.M. Affoune, B.L.V. Prasad, H. Sato, T. Enoki, Y. Kaburagi, and Y. Hishiyama, *Experimental evidence of a single nano-graphene*, Chem. Phys. Lett. 348 (2001), p. 17.

[12] H. Shioyama, *Cleavage of graphite to graphene*, J. Mat. Sci. Lett. 20 (2001), p. 499.

[13] H. Hiura, T.W. Ebbesen, K.F.J. Tanigaki, and T. Takada, *Role of* sp^3 *defect structures in graphite and carbon nanotubes*, Nature 367 (1994), p. 148.

[14] H.V. Roy, C. Kallinger, and K. Sattler, *Study of single and multiple foldings of graphitic sheets*, Surf. Sci. 407 (1998), p. 1.

[15] H.V. Roy, C. Kallinger, B. Marsen, and K. Sattler, *Manipulation of graphitic sheets using a tunneling microscope*, J. Appl. Phys. 83 (1998), p. 4695.

[16] A.N. Kolmogorov and V.H. Crespi, *Smoothest bearings: Interlayer sliding in multiwalled carbon nanotubes*, Phys. Rev. Lett. 85 (2000), p. 4727.

[17] A.N. Kolmogorov, V.H. Crespi, M.H. Schleier-Smith, and J.C. Ellenbogen, *Nanotube–substrate interactions: Distinguishing carbon nanotubes by the helical angle*, Phys. Rev. Lett. 92 (2004), p. 085503.

[18] A.N. Kolmogorov and V.H. Crespi, *Registry-dependent interlayer potential for graphitic systems*, Phys. Rev. B 71 (2005), p. 235415.

[19] S. Paulson, A. Helser, and M. Nardelli, *Tunable resistance of a carbon nanotube graphite interface*, Science 290 (2000), p. 1742.

[20] W.L. Guo and Y.F. Guo, *Energy optimum chiralities of multiwalled carbon nanotubes*, J. Am. Chem. Soc. 129 (2007), p. 2730.

[21] G.Y. Zhang, X.D. Bai, E.G. Wang, Y. Guo, and W. Guo, *Monochiral tubular graphite cones formed by radial layer-by-layer growth*, Phys. Rev. B 71 (2005), p. 113411.

[22] W.L. Guo and H.J. Gao, *Optimized bearing and interlayer friction in multiwalled carbon nanotubes*, Comput. Model. Eng. Sci. 7 (2004), p. 19.

[23] D.W. Brenner, O.A. Shenderova, J.A. Harrison, S.J. Stuart, B. Ni, and S.B. Sinnott, *A second-generation reactive empirical bond order (REBO) potential energy expression for hydrocarbons*, J. Phys. Condens. Matter 14 (2002), p. 783.

[24] L.A. Girifalco and R.A. Lad, *Compressibility and the potential energy functions of the graphite system*, J. Chem. Phys. 25 (1956), p. 693.

[25] L.X. Benedict, N.G. Chopra, M.L. Cohen, A. Zettl, S.G. Louie, and V.H. Crespi, *Microscopic determination of the interlayer binding energy in graphite*, Chem. Phys. Lett. 286 (1998), p. 490.

[26] R. Zacharia, H. Ulbricht, and T. Hertel, *Interlayer cohesive energy of graphite from thermal desorption of polyaromatic hydrocarbons*, Phys. Rev. B 69 (2004), p. 155406.